

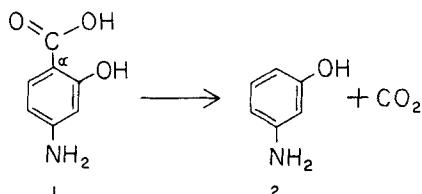
Mechanism of Decarboxylation of *p*-Aminosalicylic Acid

S. G. JIVANI AND V. J. STELLA^x

Received April 24, 1985, from the Department of Pharmaceutical Chemistry, The University of Kansas, Lawrence, KS 66045. Accepted for publication August 19, 1985.

Abstract □ The rate of decarboxylation of *p*-aminosalicylic acid (1) in aqueous solutions was studied at 25°C ($\mu = 0.5$) as a function of pH and buffer concentration. A pH-rate profile was generated by using the rate constants extrapolated to zero buffer concentration. The profile was bell-shaped, with the maximum rate of decarboxylation near the isoelectric pH. The rate constants obtained in buffered solutions indicated general acid catalysis. Bronsted behavior appeared to be adhered to. The two ionization constants of 1 were determined spectrophotometrically at 25°C and at an ionic strength of 0.5. An HPLC method was used to characterize the degradation products of the reaction. Kinetic solvent deuterium isotope effects were studied to further confirm the mechanism of decarboxylation. Below pH 7.0, the mechanism of 1 decarboxylation is the rate controlling proton attack on the carbon- α to the carboxylic acid group of 1 anion and the ampholyte, followed by the rapid decarboxylation of the formed intermediate.

The objective of this study was to investigate the mechanism of decarboxylation of *p*-aminosalicylic acid (1). The most likely decomposition reaction in the pH region below pH 10¹ is defined in Scheme I.

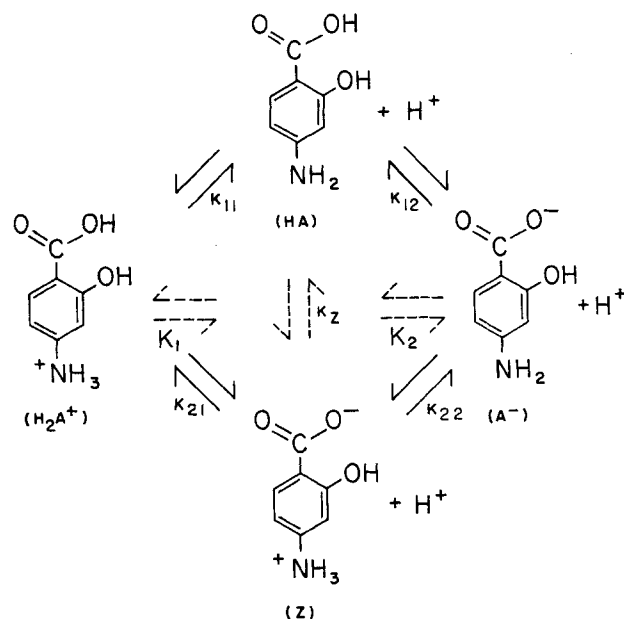
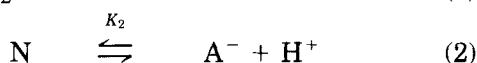
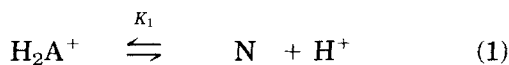


Scheme I

The interpretation of the kinetics of 1 decarboxylation in aqueous solutions is complicated by the fact that 1 and similar acids can exist as neutral, zwitterionic, cationic, and anionic forms in aqueous solution, depending on the pH of the solution, and any one or more of these forms could decarboxylate. The concentration of each species in solution varies with pH, temperature, and ionic strength; consequently, the rates of decarboxylation will vary depending on these conditions. Such variations have been used to indicate the nature of the species undergoing decarboxylation. The ionization scheme for 1 at pH values less than 7 can be defined by Scheme II.

If the concentrations of HA and Z are represented by [HA] and [Z], then the concentration of the total ampholyte, [N], is equal to the sum of [HA] and [Z]. For most purposes, N can be treated as a single species, since the ratio of zwitterion to neutral molecule is independent of pH.

The macroscopic constants K_1 and K_2 , shown in Scheme II, are defined in Eq. 1 and 2, and the microscopic constants k_{11} , k_{12} , k_{21} , and k_{22} are defined by eq. 3 and 4:



Scheme II



The individual macroscopic constants are related to the microscopic constants as follows:

$$K_1 = k_{11} + k_{21} \quad (5)$$

$$1/K_2 = 1/k_{12} + 1/k_{22} \quad (6)$$

The concentrations of each individual Bjerrum species² can be obtained by following relationships:

$$\text{H}_2\text{A}^+ = \frac{[\text{H}^+]^2}{[\text{H}^+]^2 + K_1[\text{H}^+] + K_1K_2} [\text{1}]_t \quad (7)$$

$$\text{N} = \frac{K_1[\text{H}^+]}{[\text{H}^+]^2 + K_1[\text{H}^+] + K_1K_2} [\text{1}]_t \quad (8)$$

$$\text{A}^- = \frac{K_1K_2}{[\text{H}^+]^2 + K_1[\text{H}^+] + K_1K_2} [\text{1}]_t \quad (9)$$

where $[\text{1}]_t$ is the total concentration of 1.

In solution, $[\text{H}_2\text{A}^+]$ and $[\text{A}^-]$ approach $[\text{1}]_t$ at high and low hydrogen ion concentrations, respectively, and $[\text{N}]$ reaches a maximum when $[\text{H}^+]$ equals $(K_1K_2)^{1/2}$. This corresponds to a pH equal to the isoelectric pH, pI, and is equal to $(pK_1 + pK_2)/2$.

In principle any of the four forms of **1** could be involved in the decarboxylation reaction, and the rate of decarboxylation should be greatest at the pH where the concentration of the most labile form is greatest. If the rate-controlling step in the decarboxylation of **1** is the first-order decomposition of any Bjerrum species or rate-limiting proton addition to any Bjerrum species followed by its rapid decarboxylation, a plot of the observed rate constants at zero buffer concentration versus pH should show inflections corresponding to the change in concentration of that species as a function of pH.

The kinetics of decarboxylation of **1** and similar acids have been extensively studied in the past by other workers.^{1,3-10} In all of these previous studies, the mechanism of decarboxylation was inferred from the pH dependency of the reaction along with chemical intuition and, in one case, from a structure reactivity study.¹⁰ Other mechanistic probes, such as the presence of buffer catalysis and isotope studies, were minimally used to delineate the mechanism.

Past studies of **1** decarboxylation have shown that the maximum rate of decarboxylation occurs near the pI of **1**. This rate maximum shifts to the lower pH as the temperature is increased. Above pH 10, **1** undergoes hydroxyl-ion catalyzed decarboxylation.⁶ Below pH 10 it has generally been concluded that the most likely mechanism of **1** decarboxylation is either spontaneous decarboxylation of the zwitterion or the rate-controlling proton attack on **1** anion followed by rapid decarboxylation. Based on the pH dependency of the reaction alone, these two mechanisms cannot be separated, since they are kinetically equivalent. Also, there appears to be a contribution to decarboxylation from either proton attack on either HA or Z or spontaneous decarboxylation of fully protonated **1** under strongly acidic conditions.³ Some doubt has been raised as to whether decarboxylation is the only reaction under these conditions.¹¹

Therefore, the purpose of this investigation, as stated earlier, was to probe the mechanism of decarboxylation of **1** with tools other than the simple pH dependence of the reaction, although the pH dependency of the reaction was studied. The reactions were carried out under carefully controlled conditions of constant temperature and ionic strength. The presence of general acid catalysis was tested for, and deuterium solvent isotope effects were used to further probe the mechanism. A complete product analysis by HPLC was used to confirm the decomposition product(s) as a function of time and pH.

Experimental Section

Materials—Sodium *p*-aminosalicylate (Sigma Chemical Co.) was recrystallized from an acetone-water mixture. Water used for kinetics was deionized, glass distilled, freshly boiled, and purged with nitrogen to displace oxygen and carbon dioxide. All glassware used for the kinetic studies was thoroughly rinsed with deionized water. All the chemicals used were American Chemical Society reagent grade.

Buffers—Buffer solutions were prepared with chloroacetic acid (Allied Chemicals) for the pH values 2.4–4.2, crystalline *d*-lactic acid (99% pure, J. T. Baker Chemicals) for pH 3.5–4.1, methoxyacetic acid (Aldrich Chemical Co.) for pH 3.5–4.0, acetic acid (Fisher Scientific Co.) for pH 4.4–4.8 and hydrochloric acid (J. T. Baker Chemicals) for pH values less than 2.0. The buffer concentration range was 0.04–0.2 M. All the buffer solutions were adjusted to a constant ionic strength of 0.5 with KCl. To prevent oxidation of **1** in aqueous solutions, buffers contained 2.5×10^{-3} M EDTA.

pH Measurements—All pH measurements were made at 25°C with an Orion Research model 701 digital pH meter. The pH meter was standardized with standard buffers (Fisher Scientific). Measured pH values were reproducible to ± 0.003 pH units and are assumed to be accurate to ± 0.01 units.

Methods—Determination of Ionization Constants—The two macroscopic ionization constants of **1** were determined spectrophotometrically at 25°C ($\mu = 0.5$). Solutions of **1** (10^{-4} M) at 25°C and at various

pH values in the range of 0.61–5.84 were prepared with 0.04 M acetate buffer and hydrochloric acid. A Zeiss spectrophotometer, model PM6, with a thermostated cell holder maintained at $25.0 \pm 0.5^\circ\text{C}$ was used. The appropriate buffer solution in a matched cell was used as a blank. Absorbance was read at five different wavelengths in the range of 250–270 nm. The two macroscopic ionization constants were calculated by fitting the data to the following expression:

$$A_{\text{pH}} = (A_{1^-} [\text{H}^+]^2 + A_{\text{N}} K_1 [\text{H}^+] + A_{1^-} K_1 K_2) / D \quad (10)$$

where $D = [\text{H}^+]^2 + K_1 [\text{H}^+] + K_1 K_2$; A_{pH} is absorbance at any pH; A_{1^+} , A_{N} , and A_{1^-} are the absorbances of **1** in its cationic, ampholyte, and anionic forms, respectively; K_1 and K_2 are the two ionization constants; and $[\text{H}^+]$ is the hydrogen ion concentration.

The ionization constants for the buffers were determined by titrating a 10^{-2} M solution of the acid form of the buffer against 0.5 M NaOH ($\mu = 0.5$ with KCl). The ionization constants were calculated from the titration data using the method of Albert and Serjeant.¹²

Product Analysis—Past studies¹¹ have reported that besides *m*-aminophenol (and carbon dioxide), resorcinol and 2,4-dihydroxybenzoic acid may be possible decomposition products of **1**. An HPLC method was therefore developed to separate these possible degradation products from **1** itself. Separation was accomplished at ambient temperature (25°C). Conditions for the HPLC analysis were as follows: column, ODS Hypersil 5 μm , 15 cm in length; pump, Altex 110A; injector, Water Associates U6K injector; detector, Water Associates 440 at 280 nm; flow rate, 2.0 mL/min; range, 0.20; chart speed, 5 cm/min; injection volume, 20 μL ; retention volumes, **1** (0.9 mL), *m*-aminophenol (0.24 mL), resorcinol (0.4 mL), resorcylic acid (2.68 mL); mobile phase, 55 parts methanol, 45 parts 0.05 M phosphate buffer (pH 7.0) containing 1 mM tetraoctylammonium bromide as an ion-pairing agent.

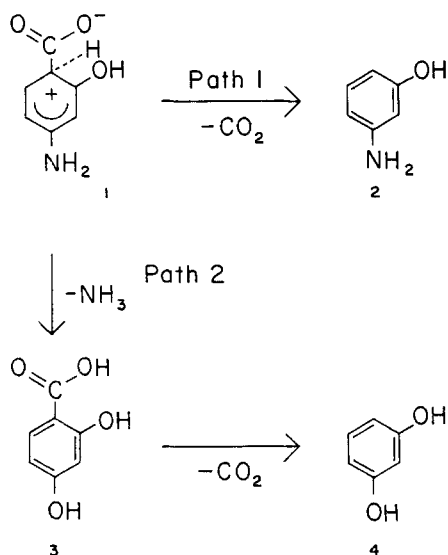
Mixtures of 10^{-4} M **1** at various pH values (pH 1.0–5.0) were followed at 25°C. Mixtures were sampled and analyzed at times corresponding to 10, 25, 50, and 75% reaction.

Rate Measurements—The change in the concentration of **1** with the time at various buffer concentrations and pH values was followed by using a spectrophotometric method.¹ Specifically, 50 mL of 3×10^{-4} M **1** in an appropriate buffer were freshly prepared. The mixtures were then maintained at $25.0 \pm 0.5^\circ\text{C}$ in a temperature-controlled water bath. The mixtures were sampled at time zero and at the predetermined time intervals. One-milliliter aliquots of the mixture were withdrawn and diluted with 2 mL of 0.5 M sodium citrate solution, to raise the pH of the solution to \sim pH 6.7. The absorbance at 300 nm (absorbance of reaction products negligible at this wavelength) was followed for approximately six to seven half-lives. The pH of the mixture was measured at various times during the run and at the end of the run and was found to be within 0.005 units of the initial pH values. Samples were refrigerated until analyzed. By raising the pH of the solution and storing the samples in a refrigerator, it was found that there was no significant further decomposition of **1** when analyzed before 3–4 days. The absorbance of the solutions at 300 nm were determined on a Perkin Elmer Lambda 1 UV/VIS spectrophotometer. Plots of the logarithm of the absorbance change against the time gave excellent linear fits.

Deuterium Solvent Isotope Effect Studies—Deuterium solvent isotope studies were undertaken as a further probe of the mechanism of decarboxylation of **1**. The kinetics of **1** decarboxylation in D_2O were followed similarly to those in H_2O . Buffers used were deuterium hydrochloride (Sigma Chemical Co.) and 0.04 M acetate buffer in deuterium oxide (Stohler Chemicals). The pH values studied were 1.1, 2.1, 3.1, 3.9, and 4.6, corresponding pD readings of 1.5, 2.5, 3.5, 4.3, and 5.0. Solutions of 3×10^{-4} M **1** in the deuterated solvents were maintained at $25.0 \pm 0.5^\circ\text{C}$ ($\mu = 0.5$ with KCl). Change in the concentration of **1** was followed spectrophotometrically at 300 nm by a procedure identical to that used for the H_2O studies.

Results

Product Analysis—The two possible routes of **1** decomposition in the aqueous solutions are shown in scheme III. After proton attack on **1** anion, the intermediate formed either undergoes rapid decarboxylation to give *m*-aminophenol (**2**)¹ or deamination to give 2,4-dihydroxybenzoic acid (**3**), which can subsequently decarboxylate to resorcinol (**4**).¹¹ The degradation products of the reaction at various pH values were



analyzed by HPLC. Figure 1A shows an HPLC chromatogram obtained for the separation of all four compounds shown in scheme III. Figure 1B shows a typical chromatogram obtained for 75% 1 decomposition at pH 1.0, showing only two peaks, 1 and 2. For all reactions at all pH values these were the only two peaks observed. From these results it is evident that 2 and carbon dioxide are the only degradation products of 1 decomposition in the pH range of 1–5.

Ionization Constants—The macroscopic ionization constants of 1 at 25°C and ionic strength of 0.5 were determined spectrophotometrically and, for the buffers, titrimetrically.

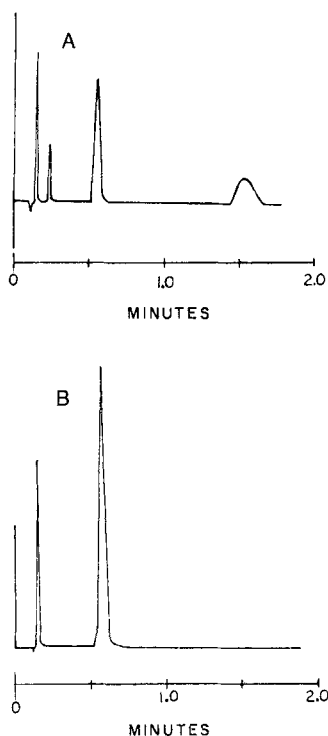


Figure 1—(A) HPLC chromatogram for the separation of m-aminophenol, resorcinol, p-aminosalicylic acid (1), and 2,4-dihydroxybenzoic acid. (B) Typical chromatogram for the 1 decomposition reaction between pH 1–5. Shown is a 75% reaction of 1 in hydrochloric acid buffer at pH 1.0.

The ionization constants of 1 at 25°C, $\mu = 0.5$, were as follows: $K_1 = 1.58 \pm 0.18 \times 10^{-2}$; $K_2 = 2.51 \pm 0.51 \times 10^{-4}$; $pK_1 = 1.80 \pm 0.04$; $pK_2 = 3.60 \pm 0.07$. Table I reports the K and pK_a values with their standard deviations for the buffers.

Rates of Decarboxylation—Rate constants for the decomposition of 1 were obtained by fitting the spectrophotometric data to eq. 11:

$$\ln(A - A^\infty) = \ln(A_0 - A^\infty) - kt \quad (11)$$

where A is the absorbance at time t , A_0 is the absorbance at time zero, and A^∞ (0.010) is the absorbance at t_∞ . Figure 2 shows representative plots of $\ln(A - A^\infty)$ versus time. The slope of such a line allows the calculation of the observed rate constant k_{obs} . Excellent straight lines were obtained confirming that 1 decarboxylation was indeed first-order. The slopes of the plots were obtained by linear regression by the method of least squares. In most cases the correlation coefficient was >0.998 . Rate constants were obtained for different reactions at a constant temperature (25°C) and ionic strength ($\mu = 0.5$) but at varying buffer concentrations and pH values. Table II lists the values of the observed rate constants with their standard deviations. The observed pseudo-first-order rate constants, when plotted against total buffer concentrations at constant pH, gave linear plots. Figure 3 shows typical plots for the chloroacetic acid buffer run at pH values of 2.4–4.2. The slopes of these lines represent the second-order catalytic rate constants, k_{cat} . The lines extrapolated to zero buffer

Table I—Ionization Constants for the Buffers (Acid Form) at 25°C, $\mu = 0.5^a$

Buffer	$K_a \times 10^3$	pK_a
Chloroacetic acid	2.090 ± 0.050	2.68 ± 0.01
Lactic acid	0.460 ± 0.010	3.34 ± 0.01
Methoxyacetic acid	0.400 ± 0.010	3.40 ± 0.01
Acetic acid	0.029 ± 0.001	4.54 ± 0.01

^a Results are means \pm standard deviations.

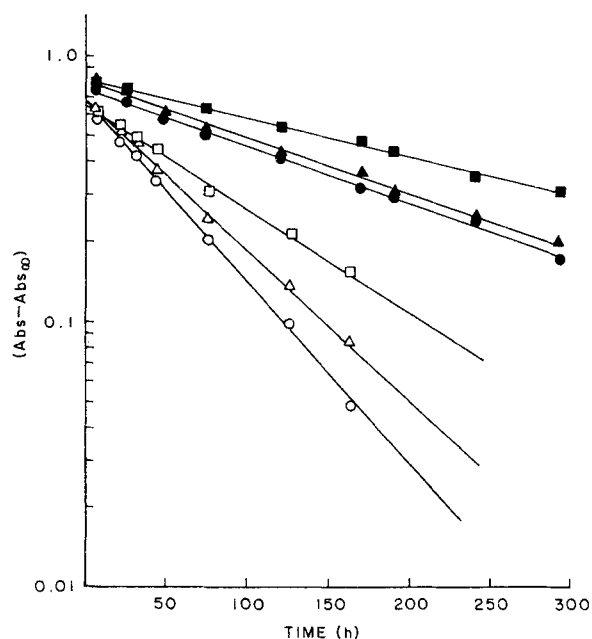


Figure 2—Aqueous decarboxylation of p-aminosalicylic acid (1) at 25°C, $\mu = 0.50$. Semilogarithmic plot of absorbance change against time, for 1 decarboxylation in 0.04 M methoxyacetic acetate buffer, at pH 3.5 (○), 3.75 (△), 4.0 (□), and 0.04 M acetate buffer at pH 4.4 (●), 4.6 (▲), and 4.8 (■).

Table II—Decarboxylation Rates of *p*-Aminosalicylic Acid in Buffer Solutions at 25°C, $\mu = 0.5$

Buffer	pH	Buffer conc., mol/L	$k_{\text{obs}} \times 10^2, \text{h}^{-1} \text{ } ^a$	Buffer	pH	Buffer conc., mol/L	$k_{\text{obs}} \times 10^2, \text{h}^{-1} \text{ } ^a$	
Chloroacetic acid	2.4	0.04	1.61 ± 0.05	Methoxyacetic acid	3.5	0.04	1.51 ± 0.05	
		0.06	1.64 ± 0.10			0.06	1.55 ± 0.08	
		0.10	1.73 ± 0.10			0.10	1.59 ± 0.07	
		0.15	1.81 ± 0.01			0.15	1.62 ± 0.05	
		0.20	1.98 ± 0.02			0.20	1.66 ± 0.03	
	2.8	0.04	1.56 ± 0.10		3.75	0.04	1.19 ± 0.04	
		0.06	1.69 ± 0.10			0.06	1.21 ± 0.05	
		0.10	1.78 ± 0.02			0.10	1.27 ± 0.05	
		0.15	1.83 ± 0.05			0.15	1.28 ± 0.03	
		0.20	1.95 ± 0.04			0.20	1.35 ± 0.06	
	3.2	0.04	1.55 ± 0.10		4.0	0.04	0.89 ± 0.02	
		0.06	1.52 ± 0.10			0.06	0.92 ± 0.01	
		0.10	1.60 ± 0.10			0.10	0.95 ± 0.03	
		0.15	1.65 ± 0.10			0.15	0.99 ± 0.03	
		0.20	1.71 ± 0.10			0.20	1.05 ± 0.06	
	3.8	0.04	0.93 ± 0.08		Acetic Acid	4.4	0.04	0.43 ± 0.07
		0.06	0.98 ± 0.03				0.06	0.47 ± 0.09
		0.10	1.01 ± 0.05				0.10	0.52 ± 0.10
		0.15	1.03 ± 0.05				0.15	0.58 ± 0.10
		0.20	1.09 ± 0.07				0.20	0.61 ± 0.10
4.2	0.04	0.49 ± 0.05	Lactic Acid	3.5	0.04	1.42 ± 0.10		
	0.06	0.62 ± 0.02			0.06	1.45 ± 0.10		
	0.10	0.65 ± 0.02			0.10	1.53 ± 0.10		
	0.15	0.65 ± 0.02			0.15	1.60 ± 0.10		
	0.20	0.66 ± 0.04			0.20	1.69 ± 0.10		
4.6	0.04	0.35 ± 0.10	3.7	0.04	1.18 ± 0.12			
	0.06	0.33 ± 0.06		0.06	1.23 ± 0.10			
	0.10	0.34 ± 0.09		0.10	1.34 ± 0.11			
	0.15	0.40 ± 0.06		0.15	1.42 ± 0.10			
	0.20	0.45 ± 0.06		0.20	1.46 ± 0.10			
4.8	0.04	0.23 ± 0.06	4.6	0.04	0.35 ± 0.10			
	0.06	0.25 ± 0.06		0.06	0.33 ± 0.06			
	0.10	0.29 ± 0.06		0.10	0.34 ± 0.09			
	0.15	0.30 ± 0.06		0.15	0.40 ± 0.06			
	0.20	0.33 ± 0.07		0.20	0.45 ± 0.06			

^a Results are the means ± standard deviations.

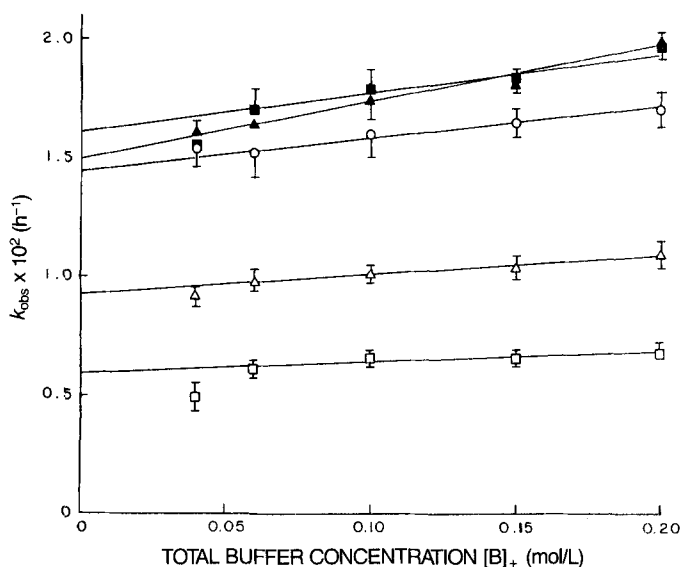


Figure 3—Dependence of rate constants of decarboxylation of *p*-aminosalicylic acid (1) at 25°C, $\mu = 0.50$, on the buffer concentration and pH of the solution. Decarboxylation of 1 in chloroacetate buffer at pH 2.4 (\blacktriangle), 2.8 (\blacksquare), 3.2 (\circ), 3.8 (\triangle), and 4.2 (\square).

concentration give the values of the observed rate constants for 1 decarboxylation at zero buffer concentration, k'_{obs} , which were then used to generate the pH-rate profile. Plots similar to those shown in Fig. 3 were done for all the buffers to obtain the k_{cat} and k'_{obs} values for all buffers and pH values. Table III summarizes these results.

pH-Rate Profile—A pH-rate profile for the decarboxylation of 1 in water, as shown in Fig. 4 (solid circles), was generated by using the values of k'_{obs} . The profile obtained was approximate bell-shaped, with the maximum rate near the apparent isoelectric pH, pI. The rate of decarboxylation decreases to an apparent constant value at low pH values and drops off at higher pH values. The points are the experimental values, and the line was theoretically generated by the fit of the data to the following expression:

$$k'_{\text{obs}} = k_{\text{H}} [\text{H}^+] F_{\text{N}} + k'_{\text{H}} [\text{H}^+] F_{\text{I}^-} \quad (12)$$

where k'_{obs} is the observed rate constant at zero buffer concentration; k_{H} is the rate constant for the proton addition to 1 ampholyte, N; k'_{H} is the rate constant for the proton addition to 1 anion; F_{N} is the fraction of 1 in its ampholyte form; and F_{I^-} is the fraction of 1 in its anionic form. These fractions can be calculated by using eq. 8 and 9 by dividing the concentration of the species by the total concentration of 1.

Table III—Catalytic Rate Constants (k_{cat}) and Observed Rate Constants at Zero Buffer Concentration (k'_{obs}) for the Decarboxylation of *p*-Aminosalicylic Acid at 25°C, $\mu = 0.5^a$

Buffer	pH	$k_{\text{cat}} \times 10^2, \text{M}^{-1} \text{h}^{-1a}$	$k'_{\text{obs}} \times 10^2, \text{h}^{-1a}$
Chloroacetic acid	2.4	2.40 ± 0.01	1.50 ± 0.005
	2.8	1.80 ± 0.01	1.58 ± 0.005
	3.2	1.20 ± 0.01	1.47 ± 0.005
	3.8	0.80 ± 0.01	0.93 ± 0.004
	4.2	0.30 ± 0.01	0.60 ± 0.004
Lactic acid	3.5	1.70 ± 0.01	1.37 ± 0.005
	3.7	1.20 ± 0.01	1.13 ± 0.005
	4.1	0.80 ± 0.01	0.68 ± 0.004
Methoxyacetic acid	3.5	0.93 ± 0.01	1.48 ± 0.005
	3.75	0.73 ± 0.01	1.18 ± 0.004
	4.0	0.63 ± 0.01	0.87 ± 0.004
Acetic acid	4.4	1.00 ± 0.01	0.40 ± 0.005
	4.6	0.71 ± 0.01	0.30 ± 0.004
	4.8	0.55 ± 0.01	0.21 ± 0.004

^a Results are the means \pm standard deviations.

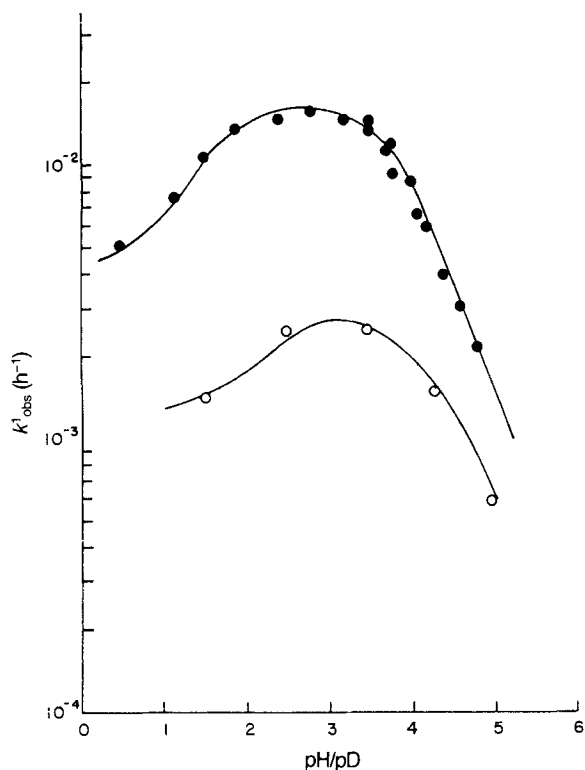


Figure 4—Dependence of the rate constants of decarboxylation of *p*-aminosalicylic acid (1) at 25°C, $\mu = 0.50$, on the pH and pD of the solutions. A plot of logarithm of rate constants versus pH (●) and pD (○) for decarboxylation of 1 in water and deuterated water.

Data were fitted to eq. 12 by the program MULTI¹³ to estimate the parameters k_{H} , k'_{H} , K_1 , and K_2 . The values for the rate constants k_{H} and k'_{H} and the pK_{a} values of 1 obtained were $k_{\text{H}} = 0.153 \pm 0.009 \text{ M}^{-1} \text{ h}^{-1}$, $k'_{\text{H}} = 150 \pm 10 \text{ M}^{-1} \text{ h}^{-1}$, $pK_{\text{a}1} = 1.6 \pm 0.1$, $pK_{\text{a}2} = 3.8 \pm 0.1$, and $\text{pI} = 2.7 \pm 0.1$.

Equation 12 is mathematically equivalent to eq. 13:

$$k'_{\text{obs}} = k_{\text{u}} F_{1^+} + k'_{\text{u}} F_{\text{N}} \quad (13)$$

where

$$k_{\text{u}} = k_{\text{H}} K_1 \quad (14)$$

$$k'_{\text{u}} = k'_{\text{H}} K_2 \quad (15)$$

and k_{u} represents the specific unimolecular rate constant for rate controlling decarboxylation of the fully protonated species, k'_{u} represents the specific unimolecular rate constant for rate-controlling decarboxylation of the ampholyte, and F_{1^+} and F_{N} are the fraction of 1 fully protonated and ampholyte species, respectively. Later discussion will suggest that the reaction scheme consistent with eq. 12 is a more likely mechanism than that defined by eq. 13.

Buffer Catalysis—By following the loss of 1 as a function of pH and buffer concentration, the presence of buffer catalysis for the decarboxylation could be verified. Plots of k_{obs} versus total buffer concentration, $[B]_{\text{t}}$, were fit to eq. 16:

$$k_{\text{obs}} = k'_{\text{obs}} + k_{\text{cat}} [B]_{\text{t}} \quad (16)$$

There is an observed significant increase in the k_{obs} with an increase in the buffer concentration, indicating the presence of buffer catalysis. The values obtained for the k_{cat} were used to analyze the presence of general acid or general base catalysis.

Normally, a typical plot of k_{cat} versus the fraction of the buffer in its acid form, F_{ha} , should be a linear with $k_{\text{cat}} = k_{\text{gb}}$ at $F_{\text{ha}} = 0.0$ and $k_{\text{cat}} = k_{\text{ga}}$ at $F_{\text{ha}} = 1.0$. For 1 decarboxylation, however, the buffer plots are likely to be more complex and possibly defined by eq. 17:

$$k_{\text{cat}} = k_{\text{ga}} F_{\text{N}} F_{\text{ha}} + k'_{\text{ga}} F_{1^-} F_{\text{ha}} + k_{\text{gb}} F_{\text{N}} F_{\text{a}^-} + k'_{\text{gb}} F_{1^-} F_{\text{a}^-} \quad (17)$$

where k_{cat} is the catalytic rate constant, k_{ga} is the general acid rate constant for the reaction of acid form of the buffer with 1 ampholyte, k'_{ga} is the general acid rate constant for the reaction of acid form of the buffer with 1 anion, k_{gb} is the general base rate constant for the reaction of anionic form of the buffer with 1 ampholyte, k'_{gb} is the general base rate constant for the reaction of anionic form of the buffer with 1 anion, F_{N} and F_{1^-} are the fraction of 1 ampholyte and anion, respectively, and F_{ha} and F_{a^-} are the fraction of the buffer in acid and anionic form, respectively.

A plot of k_{cat} versus F_{ha} may be nonlinear, as the fraction of 1 reactive species, F_{N} and F_{1^-} , are included in eq. 17. One way to estimate the general acid or base rate constants is to linearize eq. 17 by testing various approximations. From early plots of k_{cat} versus F_{ha} , it was observed that 1 decarboxylation did not appear to be subjected to a significant general base catalysis. Assuming, therefore, that there is a zero or a negligible general base catalysis, it may be possible to neglect the third and fourth terms on the right side of eq. 17 to give eq. 18:

$$k_{\text{cat}} = k_{\text{ga}} F_{\text{N}} F_{\text{ha}} + k'_{\text{ga}} F_{1^-} F_{\text{ha}} \quad (18)$$

From the pH-rate profile, k'_{H} , the rate constant for proton addition to 1 anion, is about three orders of magnitude larger than k_{H} , the rate constant for proton addition to 1 ampholyte. Assuming the same is true for the relative magnitudes of k'_{ga} and k_{ga} , it may be possible to neglect the first term in eq. 18, resulting in eq. 19:

$$k_{\text{cat}} = k'_{\text{ga}} F_{1^-} F_{\text{ha}} \quad (19)$$

Correcting k_{cat} for the fraction of 1 anion at any given pH leads to eq. 20:

$$k'_{\text{cat}} = k_{\text{cat}}/F_{1^-} = k'_{\text{ga}} F_{\text{ha}} \quad (20)$$

If all the assumptions are correct, then a plot of k'_{cat} against F_{ha} should be linear, giving k'_{ga} at $F_{ha} = 1.0$, and pass through zero at $F_{ha} = 0.0$. Figure 5 is a plot of k'_{cat} versus F_{ha} for the acetic acid buffer data. The data suggest that no general base catalysis exists, as the $F_{ha} = 0.0$ intercept is not statistically significantly different from zero. Therefore, the plot for acetic acid was fit by forcing the data through zero at $F_{ha} = 0.0$. Plots for each of the other buffers were similar, k'_{ga} values being determined from the $F_{ha} = 1.0$ intercept. Table IV is a summary of these values, and Fig. 6 is a Bronsted plot of the logarithm of k'_{ga} versus the pK_a of the buffer. The plot appears to be linear, with a slope of -0.60 .

Deuterium Solvent Isotope Effect—As a further probe of the decarboxylation of 1, the reaction was also studied in deuterium oxide. Figure 4 is the combined plot for the pH and pD profiles. There is an observed shift to the right in the pD profile due to the shift in the pK_a values of 1 in the D_2O . The downward shift in the profile is due to the decrease in the reaction rate in the deuterated solvent. The reaction proceeds approximately five times faster in water than in deuterated water. This appears to confirm that water, probably in the form of a proton addition, is involved in the rate-controlling step.

The values for k_D and k'_D were obtained by fitting the D_2O data to eq. 21:

$$k'_{obs} = k_D [D^+] F_N + k'_D [D^+] F_{I^-} \quad (21)$$

Buffer extrapolation was not done for D_2O , as at a buffer concentration of 0.04 M, minimal buffer catalysis was observed for the H_2O studies. The pK_a values for 1 were not experimentally determined in D_2O , but it has been shown by others that carboxylate and amino group pK_a values are

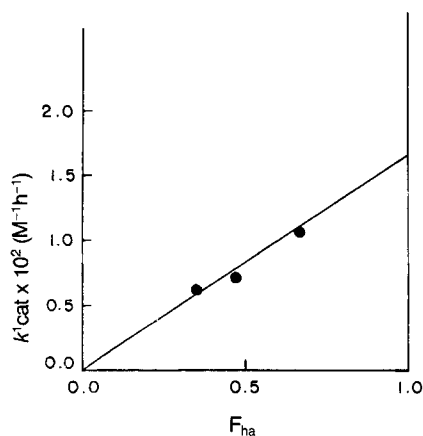


Figure 5—Dependence of catalytic rates of *p*-aminosalicylic acid (1) decarboxylation on pH of the solution. A plot of the catalytic rate constants versus the fraction of the buffer in acid form for 1 decarboxylation in acetate buffer at various pH values.

Table IV—General Acid Rate Constants for the Buffers, in Aqueous Solution Kinetics of *p*-Aminosalicylic Acid at 25°C, $\mu = 0.5$

Buffer	pK_a	pH Range	$k'_{ga} \times 10^1, M^{-1} h^{-1 a}$
Chloroacetic acid	2.68	2.4–4.2	1.00 ± 0.20
Lactic acid	3.34	3.5–4.1	0.72 ± 0.01
Methoxyacetic acid	3.40	3.5–4.0	0.39 ± 0.01
Acetic acid	4.54	4.4–4.8	0.17 ± 0.01

^a Results are the means \pm standard deviations.

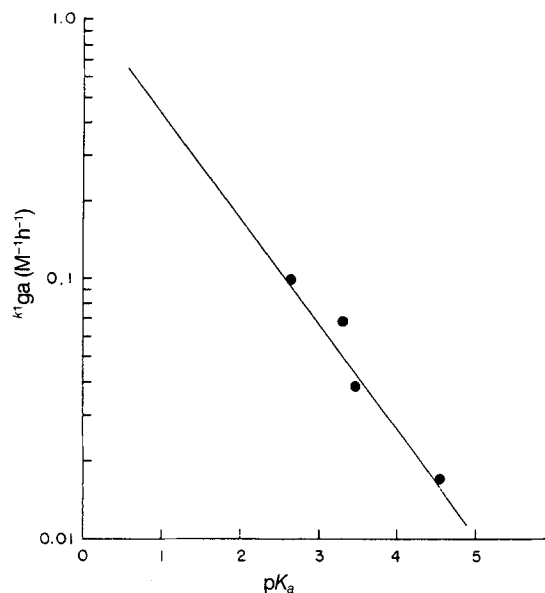
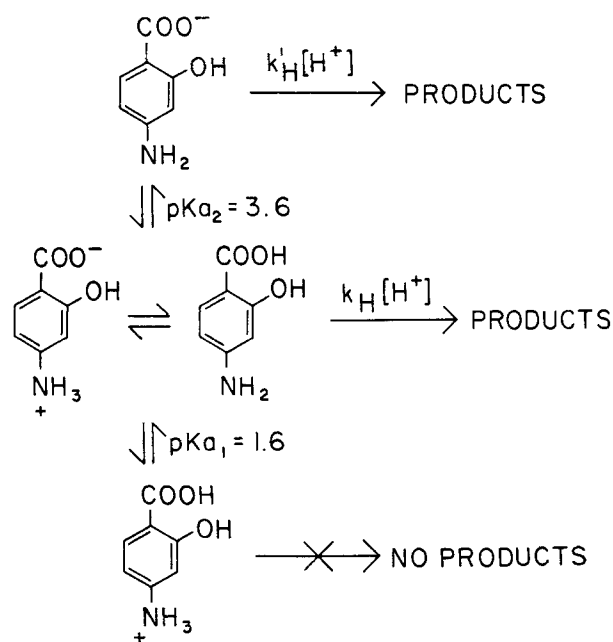


Figure 6—Bronsted relationship. A plot of logarithm of general acid rate constants versus the pK_a s of the buffer acids.

shifted upward by 0.50 pH units with the change of solvent from H_2O to D_2O .¹⁵ Values for k_D of $0.135 M^{-1} h^{-1}$ and for k'_D of $70 M^{-1} h^{-1}$ were found to adequately describe the pD-rate profile.

Discussion

The pH dependency of the decarboxylation of 1 below pH 5 is shown in Fig. 4 (solid circles). The pH-rate profile is approximately bell shaped and can be described by eq. 12 or 13. The pH dependency is consistent with the experimental observations of others.^{3-6,14} Equation 12 implies a bimolecular mechanism for 1 decarboxylation involving proton attack on 1 anion and ampholyte, N, followed by decarboxylation to give the products (Scheme IV), and eq. 13 implies a unimole-



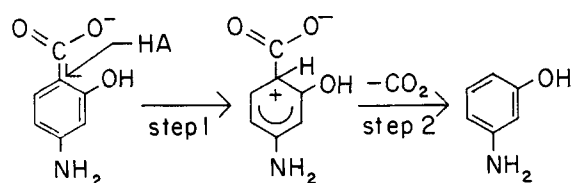
Scheme IV

cular mechanism, involving the first-order decarboxylation of the ampholyte, Z, and the cation (fully protonated species).

As stated earlier, eqs. 12 and 13 are mathematically equivalent but imply different mechanisms for 1 decarboxylation. A simple pH dependency study does not allow the differentiation of the two equations and the possible mechanisms consistent with these equations.

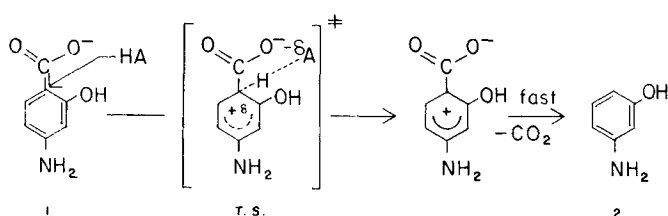
As seen from the pH profile, above pH 2.0, the major contribution to the 1 decarboxylation rate is by the second terms in the eqs. 12 and 13, whereas below this pH a major contribution to the rate is by the first terms in the equations. Thus the mechanism of decarboxylation of 1 will be discussed separately for these two pH regions.

Mechanism of Decarboxylation of 1 for pH above 2.0—The three possible mechanisms for 1 decarboxylation consistent with the second terms in the equations 12 and 13 are: (1) rate-controlling proton addition to the anion (step 1 in Scheme V) followed by rapid decarboxylation of the intermediate to give 2; (2) fast proton addition to the anion followed by rate-controlling decarboxylation of the intermediate to give 2 (step 2 in Scheme V); and (3) unimolecular decarboxylation of the zwitterion or the neutral species.



Scheme V

Since general acid catalysis was observed in this study, at pH values greater than 2.0, the most likely mechanism of those presented above is rate-controlling proton attack on the anion (bimolecular electrophilic substitution, SE_2 mechanism) followed by rapid decarboxylation of the intermediate [mechanism 1]. This observation is consistent with those in previous investigations^{16,17} on the decarboxylation of a series of substituted *o*-hydroxybenzoic acids. The Bronsted plot (Fig. 5) with a negative slope of 0.60, is consistent with a 60% transfer of a proton from the general acids to the carbon alpha to the carboxylate group in the rate controlling step. A possible transition state, TS, shown in Scheme VI.



Scheme VI

The proton addition to the carbon alpha to the carboxylate group is favored by the presence of two electron-donating groups in the *ortho* and *para* positions and also the coulombic attraction due to the presence of the carboxylate anion. This is also consistent with the findings of Brown¹⁷ on the decarboxylation of a series of substituted *o*-hydroxybenzoic acids.

Since a proton transfer appears to be the rate-controlling step, the reaction should show a significant deuterium solvent isotope effect. The observed k'_H/k'_D ratio of ~ 2.8 – 3.0 is consistent with and strongly suggestive that this is in fact the case (see Appendix). Thus, 1 undergoes decarboxylation by mechanism 1 in this pH region (Scheme VI).

Mechanism of Decarboxylation of 1 for pH below 2.0—At pH values below 2.0, the first terms in eqs. 12 and 13 contribute significantly to the observed rate constant for the decarboxylation reaction. The three most probable mechanisms are: (4) rate-controlling proton addition to the zwitterion Z or the molecular acid HA, followed by rapid decarboxylation of the intermediate to give 2; (5) fast proton addition to the zwitterion Z or the molecular acid HA followed by rate-controlling decarboxylation of the intermediate to give 2; (6) unimolecular decarboxylation of the protonated species.

Because it was not possible to determine whether general acidic catalysis was occurring at these low pH values, it was not possible to distinguish between mechanisms 4–6 on this basis. The thousand-fold decrease in the rate constant k_H relative to k'_H is consistent with the unfavored proton addition to the alpha-carbon atom. This is due to either the loss of the electron donating ability of the *p*-amino group when it becomes protonated or to the loss of the coulombic attraction contribution when the carboxylate anion becomes a carboxylic acid group.

A deuterium isotope effect is expected for either proton addition to the zwitterion or the molecular acid (mechanisms 4 and 5) or the spontaneous decarboxylation of the fully protonated species (mechanism 6). The magnitude and the direction of the expected deuterium solvent isotope effects for mechanisms 4–6 are discussed in the Appendix. The observed effect of $k_H/k_D \approx 1$ – 2 is most consistent with a proton transfer in the rate controlling step. Thus the most likely mechanism for 1 decarboxylation in this pH region is mechanism 4.

The data provided does not allow discrimination between proton addition to HA or to Z. It may be argued, on the basis of chemical intuition, that proton attack on the molecular acid HA more closely resembles the mechanism proposed at pH values above 2. The amino group in HA, being electron donating, favors the proton attack at the alpha-carbon atom. The protonated amino group in the zwitterion, Z, is electron withdrawing and does not favor the proton attack on the alpha-carbon atom. On the other hand, on the basis of coulombic effects, proton addition to the zwitterion is favored over proton addition to HA.

In summary, the mechanism of decarboxylation of 1 in the pH range of 1–5 has been evaluated. The major mechanism above pH 2 appears to be the rate-controlling proton addition to the 1 anion followed by rapid decarboxylation of the formed intermediate. At pH values below 2, the major mechanism appears to be the rate-controlling proton addition to the 1 zwitterion or the molecular acid, followed by rapid decarboxylation.

Appendix

Kinetic Solvent Isotope Effect—The term kinetic solvent isotope effect (KSIE), refers to quantitative ratio of rate constants for reactions run in light and heavy water. The magnitude of the experimentally observed KSIE provides information about the nature of transition states (T.S.) along the reaction pathway. The overall observed solvent isotope effect is the end product of all hydrogen bond interaction differences in light versus heavy water (deuterium oxide) that occur in going from the ground state, approximated by a zero point energy (ZPE), to the activated T.S.^{18–22}

Changing the hydrogen atoms of water to deuterium will bring about rate differences if either or both of the following undergo changes in going from reactant to transition state: (a) differences in bulk solvent properties and solute–solvent interactions, also called transfer or solvent effects, $(k_H/k_D)_{med}$; and (b) differences in ZPE of O—L bonds and solute bonds which arise from actual bond changes in reacting molecules. The former effect is usually taken to be negligible. Most

KSIE arise from the latter. Large and measurable KSIE are observed when a primary, $(k_H/k_D)_{\text{pri}}$, or secondary, $(k_H/k_D)_{\text{s}}$, isotope effect occurs. A primary isotope effect arises when a reaction involves rate-determining proton transfer. A secondary effect is observed when the proton is involved in the reaction but is not transferred in the rate-determining step.

The overall observed KSIE is the product of these various contributions and can be mathematically described by eq. A1:

$$(k_H/k_D)_{\text{total}} = (k_H/k_D)_{\text{pri}} (k_H/k_D)_{\text{s}} (k_H/k_D)_{\text{med}} \quad (\text{A1})$$

The purposes of measuring the KSIE are:

(a) to determine whether a proton(s) is involved in the reaction;

(b) if there is a rate determining proton transfer;

(c) to differentiate between various possible mechanisms;

(d) to gain some information about the T.S.

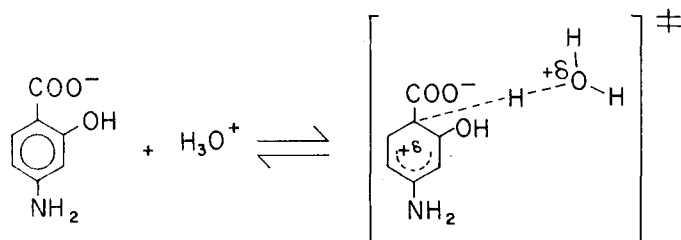
A simple method to estimate the KSIE for a reaction is by the fractionation-factor approach.¹⁸ An isotopic fractionation factor (ϕ) of any particular site in a molecule is defined as ratio of its preference for deuterium over proton relative to the similar preference of a single site in solvent molecule. The equilibrium isotope effect (K_H/K_D) is given by ratio of the ϕ values for the reactants to the products (ϕ_r/ϕ_p). The KSIE is given by the ratio of the ϕ values for the reactants to the T.S. (ϕ_r/ϕ_t). The TS fractionation-factor for sites giving secondary isotope effects is often considered to be given by:

$$\phi_t = \phi_r^{(1-x)} \phi_p^x \quad (\text{A2})$$

where x is any index of the T.S. structure, e.g., the β Bronsted value, and ϕ_r and ϕ_p are the fractionation factors of the reactant and product states, respectively.

In summary, KSIE are determined mainly by the difference in ZPE as a result of bonding changes to H (D) on going from reactant to T.S. The magnitude of this effect allows one to draw some mechanistic conclusions about the nature of the T.S. structure. For example, the fractionation-factor approach can be applied to the proposed T.S. models. One can arrive at a reasonable structure for the T.S. by comparison of the estimated solvent effects with the observed effect, and T.S. models are then accepted or rejected.

For 1, there are four species in the solution, which may undergo decarboxylation. In the pH region where 1 exists as an anion, the observed solvent isotope effect was ≈ 2.8 – 3.0 . It was postulated that proton addition to the anion, as shown, is the rate-determining step.



KSIE for the proton addition can be calculated from eq. A3:

$$k_H/k_D = \phi_r/\phi_t \quad (\text{A3})$$

In general for this mechanism, $\phi_r = (0.69)^3 = 1/3$. For a 100% transfer of the proton to the alpha-carbon atom in the transition state, $\phi_t = 1$, and therefore the expected KSIE $\approx 1/3$. This would correspond to mechanism 2 in this paper. For no transfer of the proton in the transition state, $\phi_t = (0.69)^3$, and the expected KSIE ≈ 1 . For spontaneous, unimo-

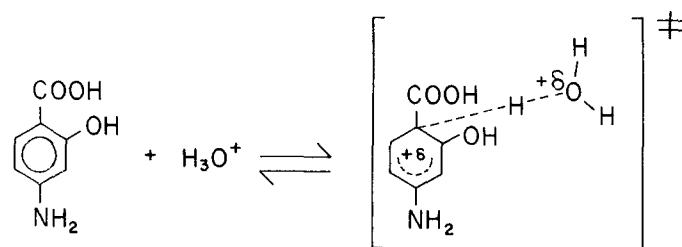
lecular decarboxylation of the zwitterion, mechanism 3, the expected KSIE is also unity. For both limiting T.S. structures, k_H/k_D is thus predicted as 1 or inverse, contrary to the observation.

For partial proton transfer of degree x , however, a primary isotope effect of up to around 7 can be expected. For larger x , ϕ_t will be closer to 1, whereas for smaller x , ϕ_t will be around $1/3$. At $x = 0.5$:

$$k_H/k_D = (0.69)^3 / [(0.69)^{0.5}]^2 [1/7] = 3.4 \quad (\text{A4})$$

This is not far from the observed effect, which is thus consistent with the model, with an intermediate value of x .

For pH values less than 2, there is a significant contribution to the observed rate from the k_H term. The observed isotope effect in this region was ≈ 1 – 2 . The postulated mechanism is rate-determining proton addition to the zwitterion or the molecular acid. Since $\phi = 1$ for all sites in both the molecular acid and the zwitterion, there will be no solvent isotope effect on their relative populations. The solvent isotope effect cannot therefore distinguish between reactions of these two species. On the basis of chemical intuition, proton attack is more favored on the molecular acid than on the zwitterion. Proton addition to the zwitterion or molecular acid is described below.



For this hypothetical mechanism:

$$k_H/k_D = \phi_r/\phi_t = (0.69)^3/\phi_t = 1/(3 \cdot \phi_t) \quad (\text{A5})$$

As before, $\phi_t = 1$ for $x = 1$ (100% proton transfer), thus predicting in an inverse solvent isotope effect for mechanisms 5 and 6. When $\phi_t = 1/3$ for $x = 0$ (0% proton transfer), no solvent isotope is predicted. Again, ϕ_t for $x = 0.5$ will lead to a k_H/k_D value of 3.4. For larger values of x , k_H/k_D will be between 3.4 and 1, and for smaller values of x , k_H/k_D will be between 3.4 and $1/3$. The observed solvent isotope effect of slightly greater than unity is thus consistent with either a smaller or a larger degree of proton transfer than was seen at higher pH values. Furthermore, proton transfer to the zwitterion or the molecular acid cannot be distinguished.

References and Notes

1. Rekker, R. F.; Nauta, W. T. *Pharm. Weekbl.* 1956, 91, 693–704.
2. Bjerrum, N. Z. *Phys. Chem.* 1923, 104, 147–157.
3. Willi, A. V.; Stocker, J. F. *Helv. Chim. Acta* 1954, 37, 1113–1121.
4. Rekker, R. F.; Nauta, W. T. *J. Med. Pharm. Chem.* 1960, 2, 281–297.
5. Liquori, A. M.; Ripamonte, A. *Gazz. Chim. Ital.* 1955, 85, 578–585.
6. Tanaka, N.; Nakagaki, M. *Yakugaku Zasshi* 1961, 81, 591–596.
7. Stevens, W. H.; Pepper, J. M.; Lounsbury, M. *Can. J. Chem.* 1952, 30, 529–540.
8. Willi, A. V. *Z. Physik. Chem. Frankfurt* 1961, 27, 221–232.
9. Dunn, G. E.; Leggate, P.; Scheffler, I. E. *Can. J. Chem.* 1965, 43, 3080–3094.
10. Willi, A. V. *J. Chem. Soc., Faraday Trans. I* 1959, 55, 433–441.
11. Thoma, V. F. *Tuberkulosearzt* 1962, 16, 362–368.
12. Albert, A.; Serjeant, E. P. in "Ionisation Constants of Acids and Bases"; T & A Constable Ltd.: Edinburgh, 1971; pp 9–22.
13. Yamaoka, K.; Tanigawara, Y.; Nakagawa, T.; Uno, T. *J. Pharm. Dyn.* 1981, 4, 879–885.

14. Rassing, J. E.; Sten Andersen, V. *Dan. Tidsskr. Farm.* **1966**, *40*, 257-275.
15. Laughton, P. M.; Robertson, R. E. in "Solvent Isotope Effects for Equilibria and Reactions in Solute-Solvent Interactions"; Coetzee, J. G.; Ritchie, C. D., Eds.; Marcel Dekker: New York, **1969**; p 407.
16. Schenkel, M.; Schenkel-Rudin, H. *Helv. Chim. Acta* **1948**, *31*, 514-524.
17. Brown, B. R.; Hammick, D. L.; Scholefield, A. J. B. *J. Chem. Soc.* **1950**, p 778-785.
18. Schowen, R. L. *Prog. Phys. Org. Chem.* **1972**, *9*, 275-332.
19. Laughton, P. M.; Robertson, R. E. in "Solute-Solvent Interactions"; Coetzee, J. F.; Ritchie, C. D., Eds.; Marcel Dekker: New York, **1969**; pp 400-538.
20. Gold, V. in "Hydrogen Bonded Solvent Systems"; Covington, A. K.; Jones, P., Eds.; Taylor and Francis, Ltd.: London, **1968**; pp 295-399.
21. "Advances in Physical Organic Chemistry," vol. 7; Gold, V., Ed.; **1969**, Academic Press: New York, **1969**; pp 259-331.
22. Arnett, E. M.; McKelvey, D. R. in "Solute-Solvent Interactions"; Coetzee, J. F.; Ritchie, C. D., Eds.; Marcel Dekker: New York, **1969**; pp 344-399.

Acknowledgments

This work was supported in part by a scholarship from the AgaKhan Foundation, Geneva to S. G. Jivani, by E. R. Squibb & Sons, and by General Research Funds from the University of Kansas.